Molecular Dynamics of the Anticodon Domain of Yeast tRNA^{Phe}: Codon-Anticodon Interaction

Ansuman Lahiri and Lennart Nilsson
Center for Structural Biochemistry, Karolinska Institutet, S 141 57 Huddinge, Sweden

ABSTRACT We have studied the effect of codon-anticodon interaction on the structure and dynamics of transfer RNAs using molecular dynamics simulations over a nanosecond time scale. From our molecular dynamical investigations of the solvated anticodon domain of yeast tRNA^{Phe} in the presence and absence of the codon trinucleotides UUC and UUU, we find that, although at a gross level the structures are quite similar for the free and the bound domains, there are small but distinct differences in certain parts of the molecule, notably near the Y37 base. Comparison of the dynamics in terms of interatomic or inter-residual distance fluctuation for the free and the bound domains showed regions of enhanced rigidity in the loop region in the presence of codons. Because fluorescence experiments suggested the existence of multiple conformers of the anticodon domain, which interconvert on a much larger time scale than our simulations, we probed the conformational space using five independent trajectories of 500 ps duration. A generalized ergodic measure analysis of the trajectories revealed that at least for this time scale, all the trajectories populated separate parts of the conformational space, indicating a need for even longer simulations or enhanced sampling of the conformational space to give an unequivocal answer to this question.

INTRODUCTION

Transfer RNA (tRNA) molecules play a major role in the translation of genetic messages. One very important step in this process is the recognition of codons. Despite being a quite large molecule, tRNAs use only three of its bases to directly interact with the codon nucleotides in the recognition process. A question that frequently arises is whether tRNA maintains a relatively rigid and passive structure in these interactions, or whether it has a dynamic structure that is modulated by different types of interactions (Labuda and Pörschke, 1980).

For the particular problem of the effect of codon-anticodon interaction on transfer RNA structure and dynamics, there are several conflicting experimental reports. From experiments with equilibrium dialysis it was concluded that formation of codon-anticodon complex triggers a conformational change in the tertiary structure of tRNA^{Phe} from E. coli, exposing the T-Ψ-C-G for binding to a base-complementary oligonucleotide C-G-A-A (Schwarz et al., 1976). Codon-dependent conformational changes were also detected in tRNA^{Phe} from yeast with fluorescent markers in the dihydrouridine loop and the anticodon loop (Y base; Robertson et al., 1977). UV absorbance measurements with tRNA^{Lys} from *Escherichia coli* showed similar results (Möller et al., 1979).

A more complex phenomenon was revealed by temperature-jump measurements using the fluorescence of the Y base of yeast tRNA^{Phe} as a natural label. Because the Y base is located at position 37 adjacent to the anticodon triplet, its fluorescence is sensitive to any changes in the conformation and the binding state of the anticodon loop. From the fluorescence study, it was inferred that tRNA may exist in solution in two conformations (Labuda and Pörschke, 1980). In fact, this same conclusion was also drawn by Ehrlich et al. (1980), who reported observations on a Mg^{2+}-dependent change in conformation in the tRNA anticodon loop as measured by the change in fluorescence intensity of the Y37 base. The binding of the codon UUC to tRNA^{Phe} occurs with more preference to one of these conformations. This seemed also to be the case for isolated anticodon loops in solution (Bujalowski et al., 1986). In another fluorescence study, Claesens and Rigler (1986) reported the observation of three possible states of the Y37 base: with low, intermediate, and high rotational mobilities. Though under normal physiological conditions Y37 was found in the low mobility state, the conformation with freely mobile Y37 was found to be the predominant one in the presence of codons.

A host of NMR studies, on the other hand, showed that the interaction of codon trinucleotides with the anticodon resulted in only minor perturbations in the structure of the RNA or the isolated anticodon domain (Geerdes et al., 1978; Davanloo et al., 1979; Clore et al., 1984).

Surprisingly, there has been very little theoretical investigation of this interesting and important problem. Although the modified nucleoside at the 37 position is not essential for tRNA^{Phe} function, experimentally it has been repeatedly demonstrated that its presence has a stabilizing effect on codon binding (Pongs and Reinwald, 1973; Wilson and Roe, 1989). Recently, Neto and coworkers have carried out quantum chemical calculations to compare the electrostatic potentials at the codon position in the presence and absence of Y37 (Werneck et al., 1998). They observed that in comparison to the substitution by a guanine base, the elec-

Received for publication 24 March 2000 and in final form 26 July 2000.

A. L.'s present address: Physical Chemistry Division, Arrhenius Laboratory, Stockholm University, S 106 91 Stockholm, Sweden.

Address reprint requests to Lennart Nilsson, Center for Structural Biochemistry, Karolinska Institutet, S 141 57 Huddinge, Sweden. E-mail: Lennart.Nilsson@csb.ki.se.

0006-3495/00/11/2276/14 $2.00

trostatic potentials on the planes containing the complementary codon bases UUC indicate a stabilization when the Y37 base is present. At the same time, they found from a semiempirical calculation significant conformational variations in the side chain of the Y base when the first uracil of codon UUC bound to A36 of the anticodon GAA (Neto et al., 1998). A hydrogen bond formation between one of the side chain carboxylic oxygens and one of the A36 amino hydrogens was suggested to impart additional strength to A·U interaction so that fidelity of the recognition between codon and anticodon improved. Sharp et al. (1990), however, found the electrostatic potentials around the anticodon region of the elongator transfer RNAs, $tRNA^{Phe}$ and $tRNA^{Asp}$, to be very similar, although they have quite different base sequences.

Whereas quantum chemical calculations for systems in vacuum do not account for an important role for water molecules in the solvation shell around the codon-anticodon complex, molecular dynamics simulations, as carried out in the present work, take care of most of the relevant interactions. Furthermore, it also gives us information about the dynamics of the system of our interest. There is a rich history of application of molecular dynamics method to study tRNA molecules, conceivably because of the early availability of high resolution structures. Initial investigations of the intramolecular dynamics of $tRNA^{Phe}$ molecule in vacuum by computer simulation were made by Harvey and coworkers (1984). Subsequent works by this group (Harvey et al., 1985; Prabhakaran et al., 1985) and others (Nilsson and Karplus, 1986) found that the main features of the crystal structure were preserved in the dynamics. In the latter work, the region studied was limited to 19 nucleotides from G26 to A44 in the anticodon domain of the yeast $tRNA^{Phe}$ molecule. It also established the fact that truncating the molecule at the anticodon stem region does not introduce any serious artifact in the structure or dynamics. On the other hand, this offered the considerable advantage of looking at an important region of the molecule at a fraction of the computational effort. Recently, Westhof and coworkers also reported a series of studies on the dynamics of fully solvated $tRNA^{Asp}$ molecules and anticodon domains (Auffinger et al., 1995, 1997).

Extracting relevant information from the wealth of data created by a molecular dynamics simulation is an area where active work is going on. Here, we look first at the root mean square (r.m.s.) deviations of the entire anticodon domain and the stem and the loop parts from the crystal structure in the presence and absence of UUC and UUU codon trinucleotides. In more detail, the residue-specific r.m.s. deviations and fluctuations were also determined from the dynamics. These quantities indicate quite clearly the general effect of codon binding on the anticodon structure and fluctuations. Behavior of the system at atomic detail was obtained from contour plots of the r.m.s. fluctuations of interatomic distances. Interest in this type of analysis has increased recently with the realization that it helps us to locate quite easily rigid subunits within a macromolecule, which in turn gives the opportunity to reduce the number of degrees of freedom that are relevant in the dynamics of the system (Genest, 1998). Here, we have constructed and compared such plots for the heavy atoms in the anticodon domain and also for the residue-averaged distances and found suggestive differences between the characteristics of the free and codon-bound anticodons.

Temperature-jump fluorescence spectroscopic observations suggested two conformational states of the anticodon domain of the tRNA molecule one of which preferentially binds the codon strand. It was postulated that these two states are the 3′-stacked as well as the 5′-stacked conformations. However, both x-ray crystallographic and NMR observations report the existence of only the 3′-stacked conformation. Molecular dynamics simulation also does not show any tendency of the system to change to a 5′-stacked form at least for a nanosecond time scale. It seems reasonable therefore that conformational alterations detected by the changes in fluorescence of the Y37 base are much less severe than supposed.

Regarding the two conformations (very likely involving the Y37 base) which interconvert with a timescale of the order of 1 ms, although it is not yet possible to explore such a slow transition with conventional molecular dynamics simulations, we attempted to detect their existence with multiple simulations by utilizing the method of generalized ergodic measure (Straub and Thirumalai, 1993). Considering two independent trajectories, α and β, we define an energy metric by first calculating the cumulative average of the energy U_i of the ith residue for both the trajectories

$$u_i^{\alpha}(t) = \frac{1}{t}\int_0^t ds U_i^{\alpha}(s) \tag{1}$$

and then calculate the metric by summing over all the N residues as

$$d_u(t) = \frac{1}{N}\sum_{i=1}^{N} \|u_i^{\alpha}(t) - u_i^{\beta}(t)\|^2. \tag{2}$$

Since $u_i(t)$ tends toward a limiting value, $d_u(t)$ should vanish for long times if the conformations visited by the trajectories mix on the time scale of the simulations. If $d_u(t)$ for long times does not vanish, then it follows that the two trajectories explore distinct conformational substates. Our results show that in the time scale of the present simulation, all the trajectories explore a different part of the phase space. It appears necessary, therefore, to enhance the phase space explorative capability of the dynamics protocol.

Computational details

The secondary structure of the yeast $tRNA^{Phe}$ anticodon domain from position 28 to 42 is given in Fig. 1. It is usual to consider two subdomains within this sequence: the stem region with a helical base-paired structure (residues 28–31 and 39–42) and a loop region consisting of the residues 32–38. The anticodon domain carries modified nucleotides at positions 32 (mC), 34 (mG), 37(Y), 39(Ψ), and 40(5mC). We developed charges and bond, angle and torsional parameters for these modified bases starting from existing CHARMM parameters for nucleic acids (version 6.5, December 1995; MacKerell et al., 1995).

The initial structure was taken from a 2.7 Å resolution crystal structure of yeast $tRNA^{Phe}$ (PDB ID: 6TNA; Sussman et al., 1978; Holbrook et al., 1978). The UUC and UUU tri-ribonucleotides were generated in the A-RNA form and manually docked to the tRNA anticodon region keeping the tRNA fixed in the crystal structure. The corresponding bases were subsequently brought to each other within hydrogen bonding distance and orientation by using distance constraints and energy minimization.

In the present calculation, Mg^{2+} located within the anticodon loop was not included because, in the preliminary runs, it was observed to give rise to a slight distortion in the structure of the anticodon nucleotides and the Y37 residue. The effect might have arisen due to the particular parameters chosen, or it might be that in the crystal this effect was suppressed by the presence of other ions and neighboring molecules. Instead, we used Na^+ ions to neutralize the negative charges on the phosphates. The Na^+ ions were placed on the bisector of the O-P-O angle, in the same plane and at a distance of around 3.5 Å from the phosphorus atoms.

All simulations were carried out using the program CHARMM (Brooks et al., 1983) version 25. After generating hydrogen atoms in the crystal structure using the HBUILD facility in CHARMM (Brunger and Karplus, 1988), the structure was subjected to 200 steps of steepest descent and 500 steps of ABNR energy minimization to eliminate short contacts. This structure was considered to be the reference structure for r.m.s deviation calculations in subsequent analyses. The molecule was then centrally placed within a 24 Å radius sphere of TIP3P water (Jorgensen et al., 1983) and all water molecules closer than 2.8 Å from RNA atoms were removed. The procedure was repeated several times, rotating the water sphere and removing the overlapping waters. The entire complex was again subjected to 200 steps of steepest descent and 500 steps of energy minimization keeping the RNA and the ions fixed. Keeping the RNA fixed, the water and ions were then thermally equilibrated at 300 K using Langevin dynamics for 20 ps with deformable stochastic boundary condition (Brooks and Karplus, 1983). The buffer region for Langevin dynamics was chosen as a shell with an inner radius of 22 Å and outer radius of 24 Å. Identical procedures were carried out for the codon-bound forms.

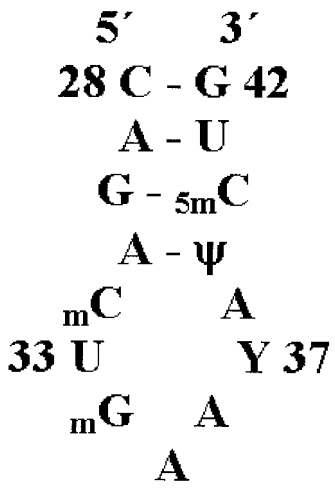

FIGURE 1 Secondary structure of yeast $tRNA^{Phe}$ anticodon domain investigated in the present simulation study.

The RNA was then gradually relaxed in two steps using harmonic constraints of 20 and 10 kcal $mol^{-1}Å^{-2}$ for 4 ps each of Langevin dynamics at 300 K, after which the complex was subjected to unrestrained dynamics except for the end basepairs. For the end basepairs, hydrogen bonding was enforced with distance constraints of 10 kcal $mol^{-1}Å^{-2}$ to prevent fraying. The stability of the simulations were judged from the absence of drift in the temperature and energies during the simulation.

In the dynamics, a time step of 2.0 fs was used and the SHAKE algorithm (Ryckaert et al., 1977) was applied to constrain the bond lengths involving hydrogen atoms to their equilibrium positions. The nonbonded pair list was updated using the heuristic algorithm in CHARMM with a 14 Å cutoff. The nonbonded interaction energies and forces were smoothly shifted to zero at 12 Å. For electrostatic calculations, a relative dielectric constant of 1.0 was used.

For multiple dynamics, we used five different runs of 500 ps duration. They differed from one another in the seeds used to generate the velocity assignments at the beginning of the equilibration step, i.e., after thermalization of the solvent. From the r.m.s. deviation profiles (Fig. 2), it is apparent that after an initial trend of divergence, they kept a steady deviation from the initial structure.

Average structure in each case was calculated over 1000 coordinate frames collected from 800 ps to 1 ns of the trajectory, after suitably orienting each of the frame. The final structures were subjected to 20 steps of steepest descent and 50 steps of ABNR energy minimization.

RESULTS AND DISCUSSION

Gross features

The question of stability and reliability of a molecular dynamics simulation was dealt with recently on the context

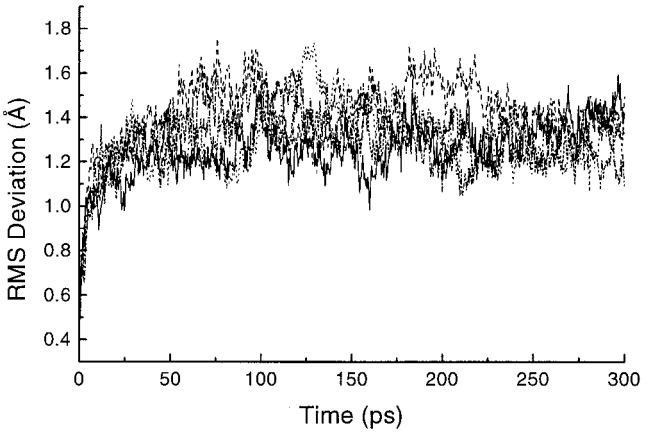

FIGURE 2 Time evolution of the r.m.s deviations of the free anticodon domain obtained from trajectories of simulations which were otherwise identical except differing in the initial velocity assignments.

of simulation of $tRNA^{Asp}$ anticodon domain (Auffinger et al., 1995). This work, in fact, provided a reexamination of the issue demonstrated earlier by Elofsson and Nilsson (1993) about the sensitive dependence of the dynamics on the initial conditions and simulation protocols. By looking at the r.m.s. deviations from the crystal structure for multiple simulations which were otherwise identical except for the initial velocity assignments, Auffinger et al. (1995) found that the structural deviations diverged appreciably from one another with time and the divergence was more pronounced for shorter ranges of nonbonded interaction between the solute and the solvent. Notably, the Ewald summation method produced trajectories which were least divergent for the time scale studied.

Although adoption of Ewald summation method in treating nonbonded interaction is generally considered to give better convergence, comparisons have shown equally stable characteristics for cutoff-based methods (Norberg and Nilsson, 2000). In the five shorter simulations with our system, we also found quite stable behavior. The average r.m.s. deviations were clustered around the value of 1.37 Å (Fig. 2). The r.m.s. deviation for the longer simulation for the free domain also did not show any increase for later time. We found that the global r.m.s. deviation quickly increased to a steady value within 100 ps and kept around that value for the entire simulation period (Fig. 3).

A related issue of interest, which arose from the divergence of almost identical simulations, is the consideration of chaos in biomolecular dynamics. Although the treatment of Auffinger et al. (1995) was not rigorous enough to determine how chaotic the dynamics was, a number of later reports measured the rate of divergence of two infinitesimally close trajectories and estimated the role of various factors on this rate (Zhou and Wang, 1996; Braxenthaler et al., 1997). Utilizing a random matrix approximation, we also showed recently that a longer cutoff in nonbonded interactions per se did not reduce the chaotic nature of the dynamics (Lahiri and Nilsson, 1999). However, fluctuations were shown to play a major role and interestingly, it appears that shorter cutoffs lead to an increased level of fluctuation in the dynamics of biomolecules (Saito, 1994).

The radius of gyration of the anticodon domain is observed to increase more slowly (Fig. 4). This is in contrast to NMR observations (Clore et al., 1984), where a relative shrinking of the molecule in solution was observed in comparison to the crystal structure. One may note that the vacuum simulation reported by Harvey et al. (1984) also observed the radius of gyration of the molecule diminishing from a value of 23.4 Å for the crystal structure to an average of 22.6 Å during the course of a 24-ps dynamics run. The shrinkage was attributed both to increased packing of atoms and to bending motions that close the angle between two

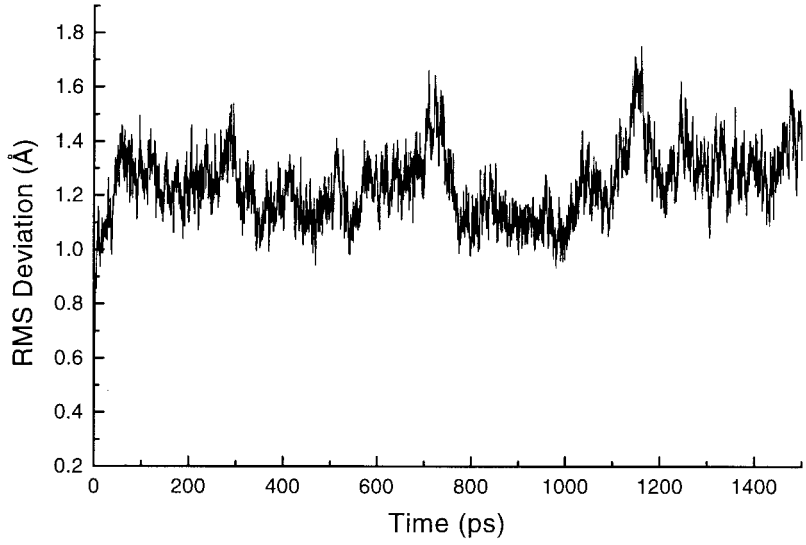

FIGURE 3 Time evolution of the r.m.s. deviation of the free anticodon domain for 1.5 ns of simulation.

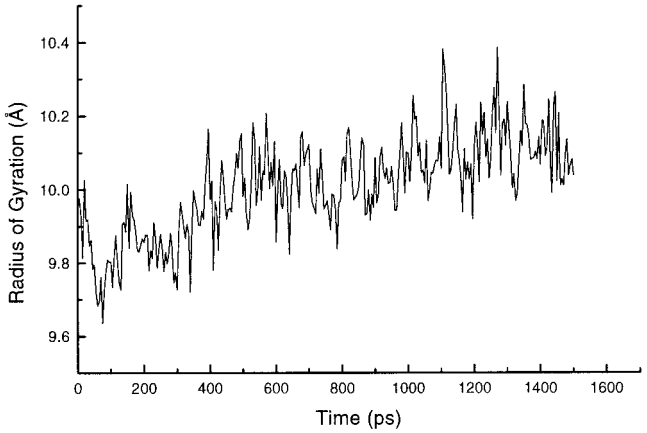

FIGURE 4 Time evolution of the radius of gyration of the free anticodon domain.

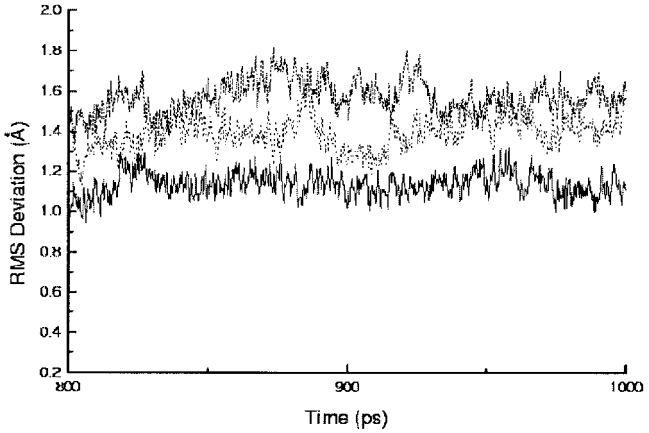

FIGURE 6 Time evolution of the r.m.s. deviations of the loop part of the anticodon domain in the free form (*solid curve*) as well as bound to the UUC codon (*dotted curve*) and the UUU codon (*dash dotted curve*) over 200 ps.

arms of the molecule. We also surmised that the increase in packing may be enhanced due to the absence of any solvent to exert outward forces on the surface atoms. The increase in the radius of gyration in our simulations might result from just such an outward attraction by the solvent atoms.

To investigate how far the binding of codons influences the global structure, we plotted the time evolution of the r.m.s. deviations of the anticodon domain bound to the UUC and UUU triplets (Fig. 5). The r.m.s. deviation profiles are seen to be similar to the free anticodon, although the deviations appear to be larger. Considering the anticodon to be composed of two substructures, one stem region and another loop, one may also consider the r.m.s. deviations of the parts separately. It turns out that the r.m.s. deviation of the stem regions remain almost the same for the free and bound anticodon domains (data not shown). However, in the presence of the codons, the r.m.s. deviations of the loop regions are considerably larger than the free anticodon (Fig. 6). Because the similarity of the magnitude of r.m.s. deviations did not rule out the structures eventually being considerably different from one another, we checked the r.m.s. deviations between the stem parts of the free and complexed anticodon with structures averaged over the last 200 ps from 1 ns runs. The results (table 1) very clearly demonstrated that the stem region retains very similar global conformation whether in the free state or bound to the codon trinucleotides. The loop region, on the other hand, shows considerable difference between the free and the bound systems.

When one looks at the deviations and fluctuations at the level of nucleotide residues and compares with the initial structure, one finds the following major common features (Fig. 7). The deviation is maximum for all the cases studied at position 32 corresponding to the base methylcytosine, the contribution of the base part being greater than that from the backbone part for this residue. There are significant deviations also in the positions of the bases Y37 and Ψ39. The end basepairs also deviate a bit with a large amount of fluctuation. In terms of mobility, the positions with the lowest amount of motion are the two nucleotides mC32 and U33. The wobble base mG34 is marked by its large amount of fluctuation. To judge the reliability of these calculations, we examined the ensemble of r.m.s. deviations and fluctuations averaged over residues obtained from five shorter simulations which gave us also an idea about the spread of these values in different simulations with almost identical initial conditions (data not shown). It was found that even

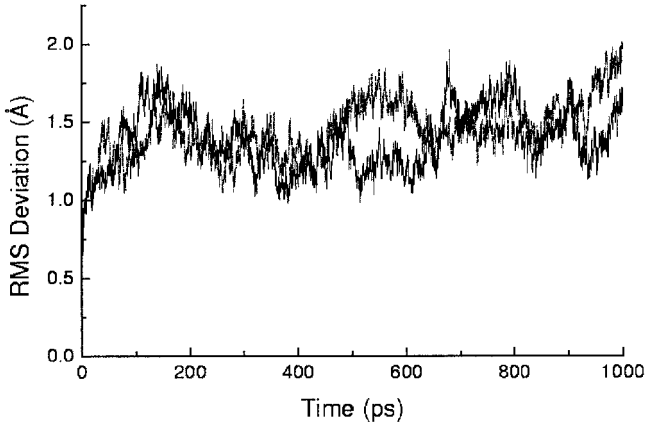

FIGURE 5 Time evolution of the r.m.s. deviations of the anticodon domain bound to the UUC and UUU codon trinucleotides.

TABLE 1 r.m.s. deviation (in Å) between the average structures from the last 200-ps runs with free anticodon (AC) and with anticodon bound to UUC and UUU codons

	AC + UUC	AC + UUU
Stem	0.45	0.62
Loop	1.12	1.18

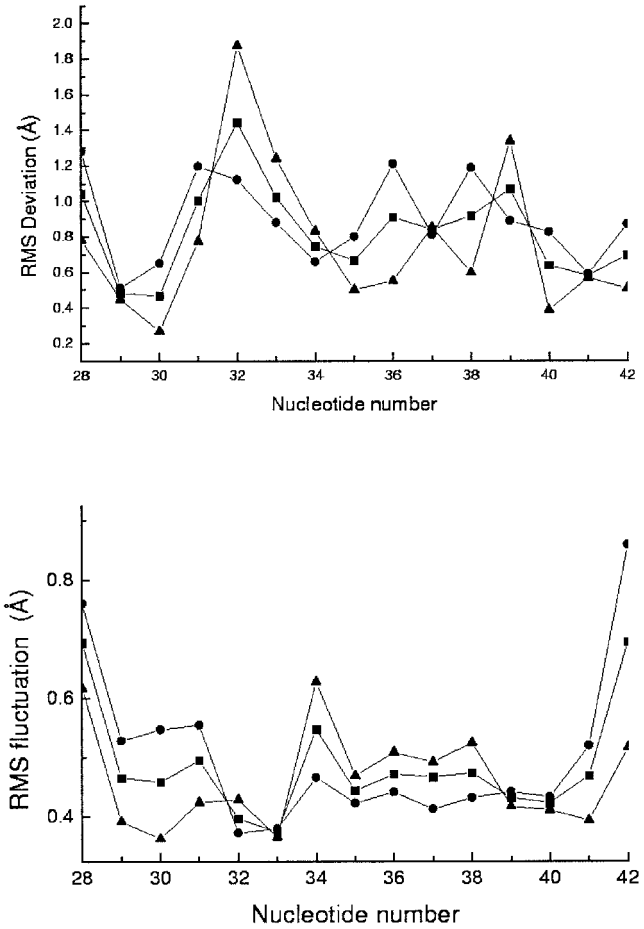

FIGURE 7 R.m.s. deviations (*top*) and r.m.s. fluctuations (*bottom*) averaged over residues for the free anticodon domain. The curves are respectively for the entire residue (*solid square*), the bases (*solid triangle*), and the backbone (*solid circle*).

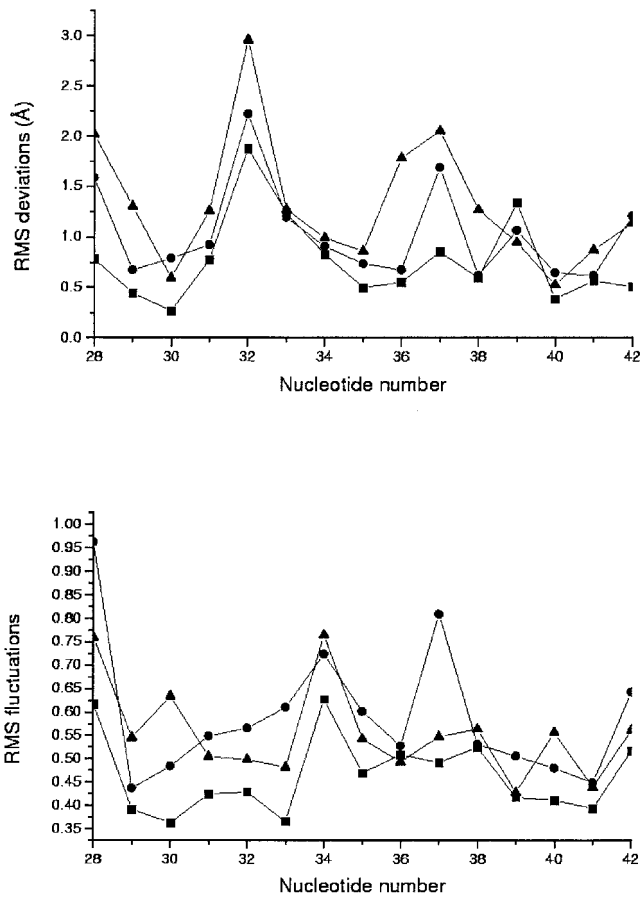

FIGURE 8 Comparison of r.m.s. deviations (*top*) and r.m.s. fluctuations (*bottom*) averaged over residues for the free anticodon domain (*solid square*) and anticodon domain bound to UUC (*solid circle*) and UUU (*solid triangle*) codon trinucleotides.

though the individual simulations did not yield identical results, the patterns were qualitatively quite similar.

A prominent feature in the comparison of the r.m.s. deviations and fluctuations averaged over residues between the free anticodon domain and the same complexed with UUC and UUU is the noticeable deviation in the Y base for the codon bound forms with respect to the free anticodon (Fig. 8). The Y base also shows increased mobility in the case where the anticodon is complexed with UUC codon.

Since a major role in base stacking is played by hydrophobic interactions, a comparison of the solvent-accessible areas (Lee and Richards, 1971) in the anticodon region may give an idea about the change in interactions in the presence and absence of codons. From Table 2, it is apparent that in the presence of codons, almost all the bases show a decrease in solvent accessibility, the base A36 being almost totally isolated from solvent. However, it is also interesting to note that interactions with the codons increases the exposed surface area of Y37 if one disregards the presence of the codon. This implies that one of the effect of the codon strand on Y37 is to draw it out more toward the solvent. The conformation, which normally would be disadvantageous, may get stabilized by stacking and/or other interactions with the codon bases.

In Table 3, we have presented the results of the global inter-base parameter analysis for the four successive nucleotides mG34-Y37 in the anticodon loop according to the Curves algorithm of Lavery and Sklenar (1988, 1989); for

TABLE 2 Comparison of the solvent-accessible surface areas (in Å^2) of the bases of the three anticodon residues and the three-ringed part of the Y37 base from 200-ps averaged structures of the free anticodon and the anticodon complexed with UUC and UUU codons

Base	AC	AC + UUC	AC + UUU
G34	132.9	86.9 (131.5)	48.6 (133.9)
A35	58.4	8.1 (65.0)	14.1 (46.3)
A36	38.8	2.8 (47.7)	4.4 (41.3)
Y37	120.6	86.3 (154.5)	82.0 (136.3)

The values within parentheses give the solvent-accessible area when one disregards the presence of codons. Probe radius = 1.6 Å.

TABLE 3 Global interbase parameters for the crystal structure and the average structures obtained from molecular dynamics simulations of the free anticodon and anticodon complexed with UUC and UUU codons

Base	Shift (Å)	Slide (Å)	Rise (Å)	Tilt (°)	Roll (°)	Twist (°)
			Crystal structure			
34/35	−1.11	−0.89	3.43	−8.78	13.84	38.93
35/36	−0.20	−1.97	3.28	6.49	7.85	16.09
36/37	−0.08	−0.46	3.52	−6.97	11.50	48.68
			Average structure of the anticodon			
34/35	−1.80	0.12	3.03	−2.27	11.68	43.51
35/36	0.17	−1.17	3.64	−4.71	7.66	33.63
36/37	−0.78	0.47	3.44	0.78	1.41	47.04
			Average structure of anticodon + UUC			
34/35	−1.38	−0.43	3.32	−0.98	12.47	43.98
35/36	−0.86	−0.86	3.61	5.83	0.43	25.43
36/37	−1.29	0.39	2.75	4.07	7.29	41.70
			Average structure of anticodon + UUU			
34/35	0.22	−0.61	3.26	−10.78	19.42	41.13
35/36	−0.59	−0.75	3.42	−1.53	1.60	27.68
36/37	0.49	−0.02	3.42	−6.75	27.48	39.82

the calculation, the entire single-stranded loop region was considered. Although the quantities in general do not show a consistent change when the parameters for the free anticodon are compared with the codon-bound forms, one finds that the twist between the bases A35 and A36 is considerably reduced in the presence of codon strands. A similar reduction in twist occurs also for the bases A36 and Y37. Fig. 9 gives stereo representations of the averaged structures for the anticodon part from simulations involving the free anticodon and the codon-bound forms showing clearly the relative disposition of the bases mG34-Y37 in the individual structures.

Fluctuations in interatomic distances

To look at the stability of the codon trinucleotides over the simulation range, we have plotted in Fig. 10, *a* and *b*, the time course of the distances between hydrogen bonding donor and acceptor atoms of the corresponding residues of the codon and anticodon parts. It was found that except for the last 200 ps in the case of wobble base pairing with UUU codon, the hydrogen bonding distances were well maintained throughout the simulation.

Fluctuations in interatomic distances were recently used to detect rigid (or quasi-rigid) subunits in proteins and nucleic acids (Nichols et al., 1995; Genest, 1998). Principal component analysis of the fluctuations in the distance matrix was recently suggested to be a better method to detect collective motions in a macromolecule (Abseher and Nilges, 1998). More recently, Matsumoto et al. (1999) observed from a normal mode analysis of the dynamics of transfer RNA that the anticodon domain as a whole behaves quite rigidly.

The evolution of the distance matrices were obtained from dynamics trajectories and the average distances as well as fluctuations were calculated over 600 ps. In Fig. 11, we present contour maps of the fluctuations in the elements of the distance matrix comprised of all the heavy atoms of the free anticodon domain. One should note here that the precise shapes of the contour maps depend on the numbering of atoms (Table 4). Since at physiological temperatures, no region in a macromolecule can be considered absolutely rigid, for finding a quasi-rigid component one has to select a tolerance level of fluctuations beyond which one does not consider the distances to be rigidly preserved. We select this level of quasi-rigidity at 0.23 following a previous investigation of the dynamics of double helical nucleic acid oligomers (Genest, 1998).

Analysis of Fig. 11 shows the result to be very similar to the dynamics observed for double stranded nucleic acid oligomers (Genest, 1998). Along the main diagonal we find a region of little fluctuation corresponding to atoms which are closely numbered and bonded to each other. Fifteen segments can be easily distinguished in this diagonal, corresponding to the 15 residues in the anticodon domain. Looking along the other diagonal, four clearly defined regions of low fluctuation can be observed. These correspond to the first four basepairs in the domain (C28-G42, A29-U41, G30–5mC40, and A31-Ψ39). Although Fig. 11 is obtained from the dynamics of the free anticodon domain, similar results were obtained for complexes with UUC and UUU codons.

In Fig. 12 we compare the interatomic distance fluctuations for the heavy atoms in the residues from mC32 to A38 for the free anticodon and with UUC and UUU codons. From the shaded regions in the contour plots which reveal distance fluctuations from 0 to 0.23, we find that there exists several islands of low fluctuation apart from the main diagonal. For the case of the free anticodon, one interesting feature comes from a subset of atoms in the low-mobility residue mC32 (atom numbers from 85 to 105). As seen in Fig. 12, a subset of atoms belonging to this residue form quasi-rigid structures with groups of atoms belonging to the neighboring low-mobility U33 residue (atom numbers from 106 to 125) and interestingly with some atoms (numbers around 204 and 225) belonging to the Y37 base. In the case of the anticodon loop bound to the codons, however, the quasi-rigid regions between mC32 and Y37 are absent. Since the rigid character of mC32 with U33 is maintained in all the three cases, it seems likely that in the presence of codons, the Y37 base fluctuates more with respect to mC32. It was observed from the contour map of average interatomic distances (not shown) that the distances between atoms in the Y37 residue and mC32 residue become greater with codon binding, consistent with the increased deviation of the Y37 residue from the crystal structure. This increased distance may be part of the reason for the increased fluctuations.

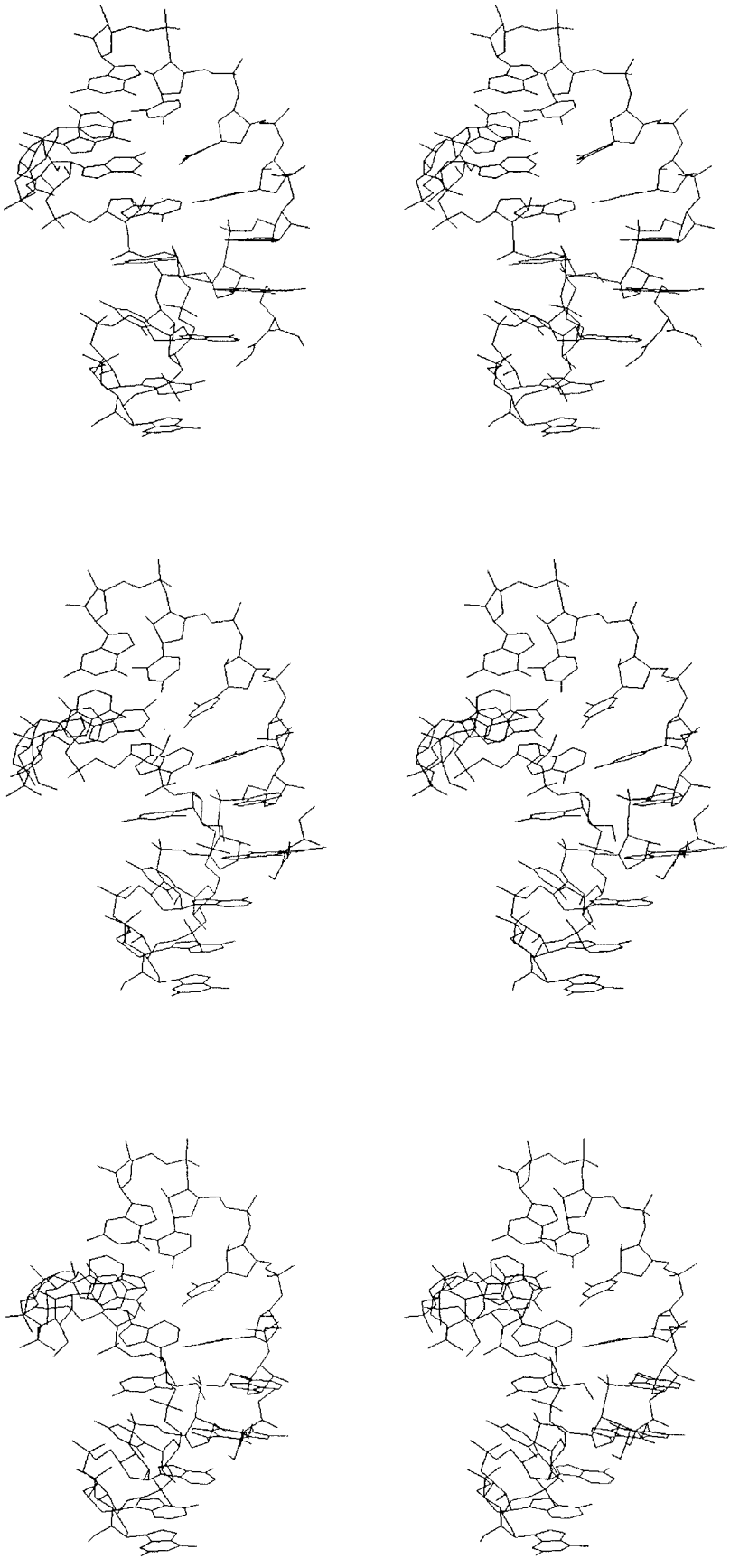

FIGURE 9 Stereo representation of the average structures of the free anticodon (*top*), the anticodon bound to the UUC codon (*middle*), and the anticodon bound to the UUU codon (*bottom*). The codon strands are not shown.

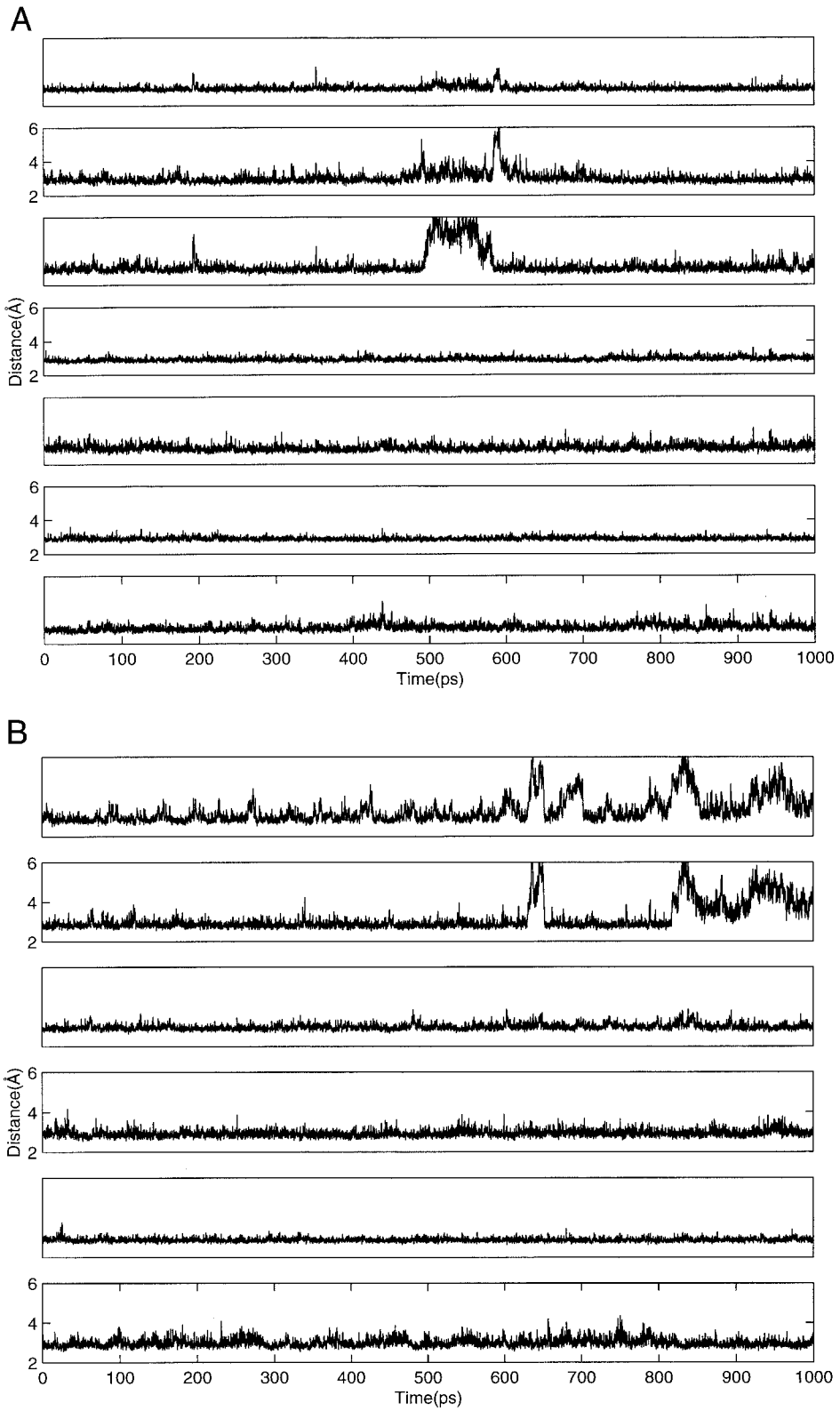

FIGURE 10 (*A*) Time evolution of the hydrogen bond distances between the codon and the anticodon bases for the anticodon-UUC complex. From the top the distances correspond to N1(mG34)-N3(C3), N2(mG34)-O_2(C3), O6(mG34)-N4(C3), N1(A35)-N3(U2), N6(A35)-O4(U2), N1(A36)-N3(U1), and N6(A36)-O4(U1). (*B*) The same for the anticodon-UUU complex. From the top the distances correspond to N1(mG34)-O_2(U3), O6(mG34)-N3(U3), N1(A35)-N3(U2), N6(A35)-O4(U2), N1(A36)-N3(U1), and N6(A36)-O4(U1), respectively. The codon nucleotides are numbered 1–3, with the first one base-pairing with A36 and the last one with mG34.

Another region of low fluctuation is comprised of subsets of atoms in the residue U33 and part of the next residue mG34 on one hand and A35 and A36 (atom numbers around 155 to 175) on the other hand. This quasi-rigid region most probably originates from stable hydrogen bonding interactions. In fact in the simulations, H3 of U33 was observed to

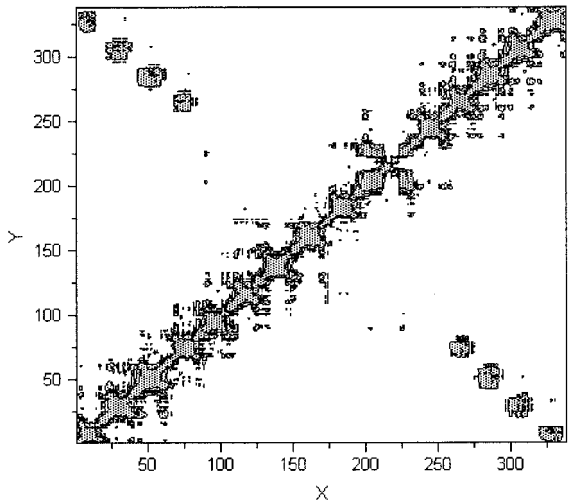

FIGURE 11 Interatomic distance fluctuation map for the heavy atoms in the free anticodon domain. Both *x*- and *y*-axes correspond to atom numbers.

make long-lived hydrogen bonds with either O1P or with O5′ of A36. U33 H2′ was also found to have hydrogen bonding with A35 N7. This also corresponds with the observation that U33 has a very low r.m.s. fluctuation. What seems interesting is that this stability in the interatomic distances in this region becomes more pronounced and spread-out in the presence of codon strands.

Comparison of residue-averaged distance fluctuation matrices also revealed interesting features (Fig. 13). The distances between residues U33 and mG34 on one hand and residues Y37, A38, and Ψ39 on the other appeared to fluctuate much more than when the codons are present.

TABLE 4 Atom numbers corresponding to base and backbone atoms in the anticodon domain

	Atom number	
Residue	Sugar-phosphate backbone	Base
C28	1–5, 14–17	6–13
A29	18–25, 36–39	26–35
G30	40–47, 59–62	48–58
A31	63–70, 81–84	71–80
mC32	85–92, 101–105	93–100
U33	106–113, 122–125	114–121
mG34	126–133, 145–149	134–144
A35	150–157, 168–171	158–167
A36	172–179, 190–193	180–189
Y37	194–201, 229–232	202–228
A38	233–240, 251–254	241–250
Ψ39	255–262, 271–274	263–270
5mC40	275–282, 292–295	283–291
U41	296–303, 312–315	304–311
G42	316–323, 335–338	324–334

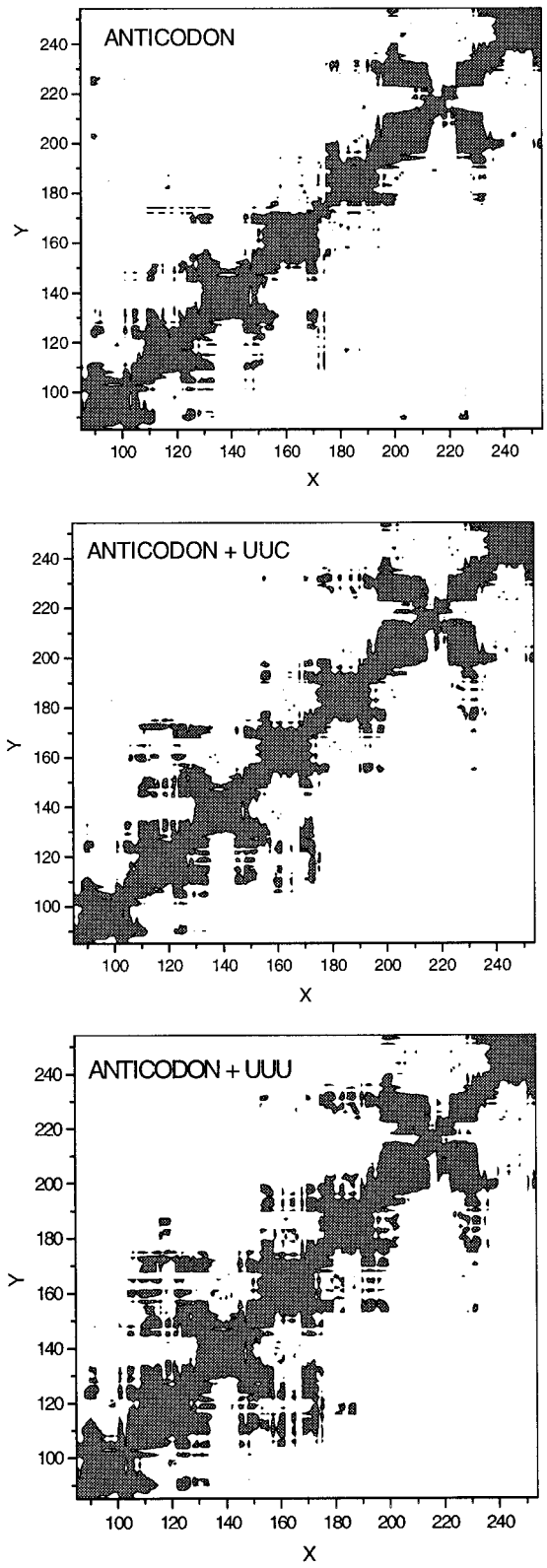

FIGURE 12 Interatomic distance fluctuation maps for the anticodon region spanning residues mC32 to A38 for the free and UUC and UUU bound anticodon (details in the text). *x*- and *y*-axes correspond to atom numbers.

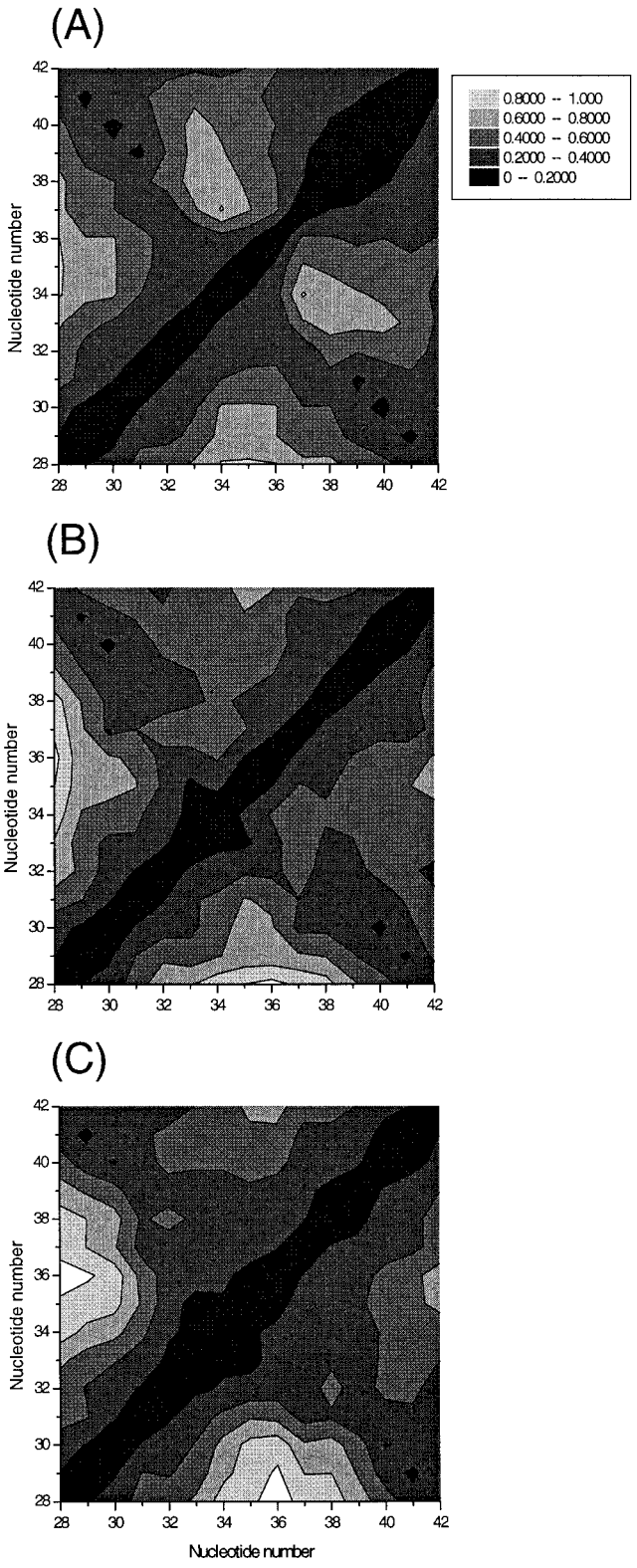

FIGURE 13 Comparison of interresidue distance fluctuation maps for (*A*) free anticodon, (*B*) anticodon bound to UUC, and (*C*) anticodon bound to UUU.

Exploration of conformational substates

Experimental results from fluorescence measurements suggested the existence of at least two conformational substates for the anticodon loop. The conformations seemed to be differentially stabilized by Mg^{2+} ion coordination and binding of the codon strand. Initially, it was thought that two conformations detected may be the 5′-stacked and the 3′-stacked conformations of the anticodon nucleotides. However, a detailed NMR study of the structure of the pentadecamer in the anticodon loop (Clore et al., 1984) failed to detect the existence of a 5′-stacked conformation. It seems possible that the conformations detected by the change in fluorescence from the Y base are not so drastically different, but differ only in the local conformation near the Y base. In that case molecular dynamics simulations may be utilized to detect and characterize such conformational changes.

The time scale of the conformational transition between the two states as reported by fluorescence data was of the order of milliseconds. The capability of molecular dynamics simulations do not extend to this time domain. However, as has been argued by different authors (Elofsson and Nilsson, 1993; Auffinger et al., 1995; Caves et al., 1998), multiple molecular dynamics simulations may have a better possibility of detecting these conformations because of their better sampling of phase space.

Here we utilize the recently proposed method of generalized ergodic measure (Straub and Thirumalai, 1993) to detect conformational substates that are separated by barriers high enough to prevent mixing during the simulation time scale. In the present case we have selected the interaction energy of one residue with the system as one possible probe of the local conformation.

In Fig. 14, we present the cumulative average of the interaction energy (vide Eq. 1) of the Y37 residue for six

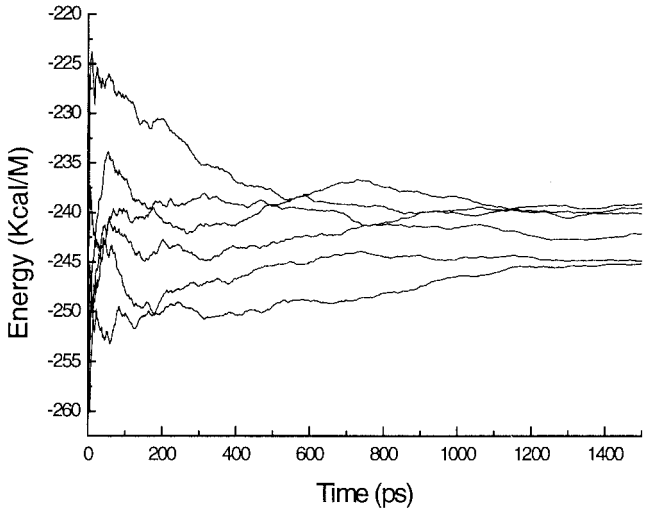

FIGURE 14 Cumulative average of the interaction energy of residue Y37 from six independent trajectories.

molecular dynamics trajectories. We assume that the interaction energy of this residue with the rest of the system reflects, in some sense, the local structure around the residue. If for different simulations, the local structure around the selected nucleotide is similar on the average, then the average interaction energy in different simulations would tend to the same value. It is clear from Fig. 14 that for our present set of simulations, the asymptotic values of the average interaction energy of Y37 cluster to three different groups. This suggests that for some of the simulations, the local environment for that residue is similar on the average. This trend is reflected in the case of all the other residues.

The situation changes, however, when we examine the global energy metric, i.e., by summing over all the residues in the anticodon domain (vide Eq. 2). In Fig. 15, we have plotted the time evolution of the energy metric for pairs of trajectories obtained from the five short simulations. For all of the cases, we find a nonzero difference for each pair of simulations. This suggests that even if a particular residue sees only a few possible local environments in different simulations, the combination of all these possibilities when we consider all of the residues together makes the trajectories diverge and populate parts of the energy landscape from where they are separated by barriers that prevent the conformations to mix within the simulation time scale.

Our result confirms a similar observation from multiple molecular dynamics simulations performed on $tRNA^{Asp}$ which investigated the hydration of the anticodon domain of the molecule (Auffinger and Westhof, 1997). From six 500-ps-long simulations that were dynamically quite similar, the authors obtained hydration patterns which were different from each other, thus locating each simulation to a separate part of the energy landscape. In our case also, we find that although locally for one particular residue the conformations seem to converge to a small number of states, when one considers the entire molecule with its solvent environment, a time scale of a few hundred picoseconds does not seem to be enough to overcome most of the barriers. To get an unequivocal answer to the problem in question, it is clearly necessary either to increase the simulation time by a few orders of magnitude or to enhance the efficiency of phase space exploration by some other technique.

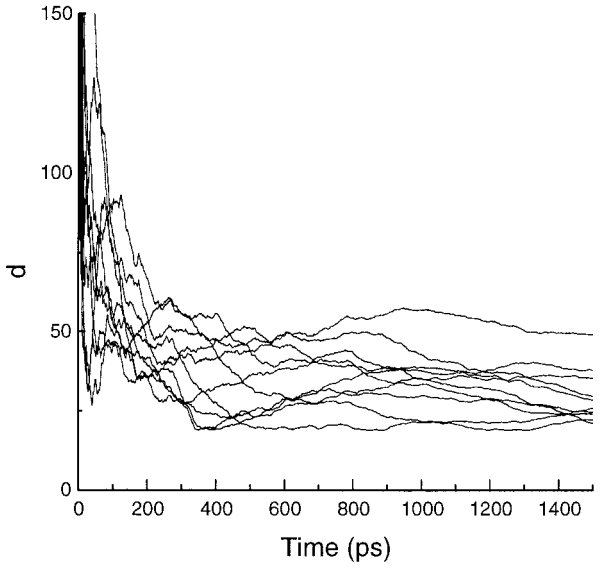

FIGURE 15 Time evolution of d_u for different pairs of trajectories from the multiple simulations.

CONCLUSIONS

We have examined the dynamical features of solvated anticodon domain of $tRNA^{Phe}$ in the presence and absence of the codon trinucleotides UUC and UUU over a nanosecond time scale. A relevant question addressed here is whether interaction with the codon trinucleotides results in a noticeable alteration in the structure and dynamics of the anticodon domain. Fluorescence spectroscopic investigations and temperature-jump measurements using the fluorescent Y37 base as a probe have detected different conformations of the anticodon loop in the free form and the codon-bound form. NMR investigations on the other hand, did not detect any significant change in the structure as a result of codon binding.

From our molecular dynamical investigations, we found stable dynamics of the anticodon domain of yeast tRNA using a long-range cutoff for nonbonded interactions and stochastic boundary conditions. The stability is manifested both in shorter multiple molecular dynamics simulations and simulations over a longer time scale in the presence and absence of codons.

From our study of the dynamics of the anticodon domain over a time scale of 1 ns, we found that in the presence of codons, the anticodon stem is the least perturbed. Structural deviation is more pronounced in the loop region, being concentrated in the conformation of the three anticodon bases and the Y37 base. Signatures of conformational differences between the codon bound and free anticodon forms were detected which generally agreed with previous fluorescence measurements and theoretical calculations. The Y37 residue was observed to deviate more from the initial structure in the codon-bound forms. Analysis of the helicoidal parameters for the four bases mG34-Y37 in the anticodon loop showed that the twist between the bases A35, A36, and Y37 becomes reduced in the presence of codons. The Y37 residue also had a greater r.m.s. fluctuation in the presence of the UUC codon. Moreover, the interatomic distances between Y37 and mC32 showed more fluctuations when the anticodon was bound to codons, whereas the distances between subsets of atoms comprising the residues U33 and mG34 on one hand and A35 and A36 on the other hand showed less fluctuation in the presence of codons.

However, our efforts to detect (using the method of generalized ergodic measure) whether $tRNA^{Phe}$ exists in solution in two different conformations, one of which binds predominantly to the codon, were frustrated by the fact that globally, all the independent simulations led to conformations that populated different regions of the conformational space. We feel that at the present state of art, conventional molecular dynamics is too limited in scope to properly resolve this interesting issue and we expect that application of some of the emerging methods to enhance the exploration of conformational space would be helpful in future.

Since we have not included in our simulations Mg^{2+} ion crystallographically located within the anticodon loop, we are unable to comment on the role of this ion in modulating the structure and dynamics of the anticodon. As in the case of $tRNA^{Asp}$ (Auffinger et al., 1995) we observe stable dynamics of the anticodon domain even in the absence of Mg^{2+} ion. Apparently, Mg^{2+} ions stabilize the tertiary structure of tRNAs by accumulating in regions of high negative electrostatic potentials, and there is not much role envisaged for specifically coordinated ions (Misra and Draper, 2000). However, a number of experimental reports point to the existence of Mg^{2+}-dependent alterations in the local structure and mobilities of nucleotides comprising the anticodon loop (Schwarz et al., 1976; Ehrlich et al., 1980; Labuda and Pörschke, 1980; Claesens and Rigler, 1986). It would be of considerable interest to address this question in future simulations.

This work was supported by the Swedish Natural Science Research Council and by the Wenner-Gren Foundation.

REFERENCES

Abseher, R., and M. Nilges. 1998. Are there non-trivial dynamic cross-correlations in proteins? *J. Mol. Biol.* 279:911–920.

Auffinger, P., S. Louise-May, and E. Westhof. 1995. Multiple molecular dynamics simulations of the anticodon loop of $tRNA^{Asp}$ in aqueous solution with counterions. *J. Am. Chem. Soc.* 117:6720–6726.

Auffinger, P., and E. Westhof. 1997. RNA hydration: 3 ns of multiple molecular dynamics simulations of the solvated $tRNA^{Asp}$ anticodon hairpin. *J. Mol. Biol.* 269:326–341.

Braxenthaler, M., R. Unger, D. Auerbach. J. A. Given, and J. Moult. 1997. Chaos in protein dynamics. *Proteins.* 29:417–425.

Brooks, B. R., R. E. Bruccoleri, B. D. Olafson, D. J. States, S. Swaminathan, and M. Karplus. 1983. CHARMM: a program for macromolecular energy, minimization, and dynamics calculations *J. Comp. Chem.* 4:187–217.

Brooks, C. L., and M. Karplus. 1983. Deformable stochastic boundaries in molecular dynamics. *J. Chem. Phys.* 78:6312–6325.

Brunger, A., and M. Karplus. 1988. Polar hydrogen positions in proteins: empirical energy function placement and neutron diffraction comparison. *Proteins.* 4:148–156.

Bujalowski, W., M. Jung, L. W. McLaughlin, and D. Pörschke. 1986. Codon-induced association of the isolated anticodon loop of $tRNA^{Phe}$. *Biochemistry.* 25:6372–6378.

Caves, L. S., J. D. Evanseck, and M. Karplus. 1998. Locally accessible conformations of proteins: multiple molecular dynamics simulations of crambin. *Protein Sci.* 7:649–666.

Claesens, F., and R. Rigler. 1986. Conformational dynamics of the anticodon loop in yeast $tRNA^{Phe}$ as sensed by the fluorescence of wybutine. *Eur. Biophys. J.* 13:331–342.

Clore, G. M., A. M. Gronenborn, E. A. Piper, L. W. McLaughlin, E. Graeser, and J. H. van Boom. 1984. The solution structure of a RNA pentadecamer comprising the anticodon loop and stem of yeast $tRNA^{Phe}$. *Biochem. J.* 221:737–751.

Davanloo, P., M. Sprinzl, and F. Cramer. 1979. Proton nuclear magnetic resonance of minor nucleosides in yeast phenylalanine transfer ribonucleic acid. Conformational changes as a consequence of aminoacylation, removal of the Y base, and codon-anticodon interaction. *Biochemistry.* 18:3189–3199.

Ehrlich, R., J.-F. Lefevre, and P. Remy. 1980. Fluorimetric study of the complex between yeast phenylalanyl-tRNA synthetase and $tRNA^{Phe}$. *Eur. J. Biochem.* 103:145–153.

Elofsson, A., and L. Nilsson. 1993. How consistent are molecular dynamics simulations? Comparing structure and dynamics in reduced and oxidized *Escherichia coli* thioredoxin. *J. Mol. Biol.* 233:766–780.

Geerdes, H. A., J. H. van Boom, and C. W. Hilbers. 1978. Codon-anticodon interaction in yeast $tRNA^{Phe}$: an 1H NMR study. *FEBS Lett.* 88:27–32.

Genest, D. 1998. Motion of groups of atoms in DNA studied by molecular dynamics simulation. *Eur. Biophys. J.* 27:283–289.

Harvey, S. C., M. Prabhakaran, B. Mao, and J. A. McCammon. 1984. Phenylalanine transfer RNA: molecular dynamics simulation *Science.* 223:1189–1191.

Harvey, S. C., M. Prabhakaran, and J. A. McCammon. 1985. Molecular-dynamics simulation of phenylalanine transfer RNA. I. Methods and general results. *Biopolymers.* 24:1169–1188.

Holbrook, S. R., J. L. Sussman, R. W. Warrant, and S.-H. Kim. 1978. Crystal structure of yeast phenylalanine transfer RNA II. Structural features and functional implications. *J. Mol. Biol.* 123:631–660.

Jorgensen, W. L., J. Chandrasekhar, J. D. Madura, R. W. Impey, and M. L. Klein. 1983. Comparison of simple potential functions for simulating liquid water. *J. Chem. Phys.* 79:926–935.

Labuda, D., and D. Pörschke. 1980. Multistep mechanism of codon recognition by transfer ribonucleic acid. *Biochemistry.* 19:3799–3805.

Lahiri, A., and L. Nilsson. 1999. Examining the charactaristics of chaos in biomolecular dynamics: a random matrix approximation. *Chem. Phys. Lett.* 311:459–466.

Lavery, R., and H. Sklenar. 1988. The definition of generalized helicoidal parameter and of axis curvature for irregular nucleic acids. *J. Biomol. Struct. Dynam.* 6:63–91.

Lavery, R., and H. Sklenar. 1989. Defining the structure of irregular nuclein acids: conventions and principles. *J. Biomol. Struct. Dynam.* 6:655–667.

Lee, B., and F. M. Richards. 1971. The interpretation of protein structures: estimation of static accessibility. *J. Mol. Biol.* 55:379–400.

MacKerell, A. D., J. Wiorkiewicz-Kuczera, and M. Karplus. 1995. An all-atom empirical energy function for the simulation of nucleic acids. *J. Am. Chem. Soc.* 117:11946–11975.

Matsumoto, A., M. Tomimoto, and N. Go. 1999. Dynamical structure of transfer RNA studied by normal mode analysis. *Eur. Biophys. J.* 28: 369–379.

Misra, V. K., and D. E. Draper. 2000. Mg^{2+} binding to tRNA revisited: the nonlinear Poisson-Boltzmann model. *J. Mol. Biol.* 299:813–825.

Möller, A., U. Wild, D. Riesner, and H. G. Gassen. 1979. Evidence from ultraviolet absorbance measurements for a codon-induced conformational change in lysine tRNA from E. coli. *Proc. Natl. Acad. Sci. USA.* 76:3266–3270.

Neto, M. D., M. S. Giambiagi, and M. Giambiagi. 1998. Influence of the hypermodified Y base on the A·U pairing in the codon-anticodon interaction. *Chem. Phys. Lett.* 290:205–210.

Nichols, W. L., G. D. Rose, L. F. Ten Eyck, and B. H. Zimm. 1995. Rigid domains in proteins: an algorithmic approach to their identification. *Proteins.* 23:38–48.

Nilsson, L., and M. Karplus. 1986. Molecular dynamics simulation of the anticodon arm of phenylalanine transfer RNA. *In* Structure and Dynamics of RNA. Plenum Press, New York. 151–159.

Norberg, J., and L. Nilsson. 2000. On the truncation of long-range electrostatic interactions in DNA. *Biophys. J.* 79:1537–1553.

Pongs, O., and E. Reinwald. 1973. Function of Y in codon-anticodon interaction of $tRNA^{Phe}$. *Biochem. Biophys. Res. Comm.* 50:357–363.

Prabhakaran, M., S. C. Harvey, and J. A. McCammon. 1985. Molecular-dynamics simulation of phenylalanine transfer RNA. II. Amplitudes, anisotropies, and anharmonicities of atomic motions. *Biopolymers.* 24: 1189–1204.

Robertson, J. M., M. Kahan, W. Wintermeyer, and H. G. Zachau. 1977. Interactions of yeast $tRNA^{Phe}$ with ribosomes of yeast and *Escherichia coli*: a fluorescence spectroscopic study. *Eur. J. Biochem.* 72:117–125.

Ryckaert, J. P., G. Ciccotti, and H. J. C. Berendsen. 1977. Numerical integration of the cartesian equations of motion of a system with constraints: molecular dynamics of n-alkanes. *J. Comput. Phys.* 23:327–341.

Saito, M. 1994. Molecular dynamics simulations of proteins in solution: artifacts caused by the cutoff approximation. *J. Chem. Phys.* 101: 4055–4061.

Schwarz, U., H. M. Menzel, and H. G. Gassen. 1976. Codon-dependent rearrangement of the three-dimensional structure of phenylalanine tRNA, exposing the T-psi-C-G sequence for binding to the 50S ribosomal subunit. *Biochemistry.* 15:2484–2490.

Sharp, K. A., B. Honig, and S. C. Harvey. 1990. Electrical potential of transfer RNAs: Codon-anticodon recognition. *Biochemistry.* 29: 340–346.

Straub, J. E., and D. Thirumalai. 1993. Exploring the energy landscape in proteins. *Proc. Natl. Acad. Sci. USA.* 90:809–813.

Sussman, J. L., S. R. Holbrook, R. W. Warrant, G. M. Church, and S.-H. Kim. 1978. Crystal structure of yeast phenylalanine transfer RNA. I. Crystallographic refinement. *J. Mol. Biol.* 123:607–630.

Werneck, A. S., M. de O. Neto, and E. R. Maia. 1998. The hypermodified Y base electrostatic contribution to the energetics of the codon-anticodon pairing in $tRNA^{Phe}$. *J. Mol. Struc. (Theochem).* 427:15–23.

Wilson, R. K., and B. A. Roe. 1989. Presence of the hypermodified nucleotide N6-(delta 2-isopentenyl)-2-methylthioadenosine prevents codon misreading by *Escherichia coli* phenylalanyl-transfer RNA. *Proc. Natl. Acad. Sci. USA.* 86:409–413.

Zhou, H., and L. Wang. 1996. Chaos in biomolecular dynamics. *J. Phys. Chem.* 100:8101–8105.